Structure Elucidation

DOI: 10.1002/anie.200803474

Structure and Dynamics of $^{13}C,^{15}N$-Labeled Lipopolysaccharides in a Membrane Mimetic**

Wei Wang, Hans Jürgen Sass, Ulrich Zähringer, and Stephan Grzesiek**

Lipopolysaccharide (LPS, endotoxin) is the major constituent of the outer leaflet within the outer membrane of Gram-negative bacteria. It represents one of the first targets by which the innate immune system recognizes bacterial infection. In small amounts, LPS provokes a beneficial stimulation of the immune system. However, in larger amounts, LPS leads to septic (endotoxic) shock,[1,2] a rapidly progressing inflammatory disease with an estimated incidence of 50–300 cases per 100000 people per year[3,4] and a mortality of 29%, even in the developed world.[4]

The complex structure of LPS consists of three major components (Figure 1): the highly variable outer O-antigen segment, a more conserved core, and the lipid A portion.[5,6] The "classic" *Escherichia coli* lipid A contains two phosphorylated glucosamine (GN) units, which are hexaacylated by four primary β-hydroxylated and two secondary non-hydroxylated fatty acids (FAs). These fatty acids constitute the hydrophobic anchor of LPS in the bacterial membrane. Lipid A is linked to the outer core part of LPS by two 3-deoxy-D-*manno*-oct-2-ulosonic acid (KD) units. The endotoxicity resides in the lipid A motif,[5] and it has been shown that both phosphates and all six fatty acids are absolutely required for the endotoxic reaction; for example, the removal of only one fatty acid from the six fatty acids of lipid A results in complete loss of the endotoxic activity.[7]

Structure information about the conformation of LPS during immune recognition and signaling events is currently lacking. At present, the only 3D structure of an intact LPS molecule that is available was obtained by X-ray crystallography in an incidental complex with the *E. coli* ferrichrome-iron receptor FhuA,[8] which has no relation to the endotoxic recognition events. Recently, crystallographic structures of MD2 in a complex with lipid IVa[9] and in a ternary complex with eritoran and TLR4[10] have also been reported. Both lipid IV_A and eritoran are well-known endotoxin antagonists[5] and have chemical structures similar to that of lipid A, but they lack two of the six fatty acid chains. None of these structures contain LPS in a membrane-associated form. Thus, the complex structures do not reveal insights into the endotoxically active conformation of LPS. Similarly to the crystallographic studies, investigations of the LPS structure in solution have been impeded by the strong tendency for the molecule to aggregate. Despite early attempts to determine the chemical structure by solution NMR spectroscopy, for example, in sodium dodecylsulfate (SDS) micelles,[11] NMR studies on the three-dimensional conformation of LPS have only been carried out on partial, synthetic lipid A molecules dissolved in dimethylsulfoxide (DMSO)[12] or in aqueous SDS micelles.[13]

In the present study, we have taken a different route to the structure and dynamics analysis of complex LPS molecules in aqueous solution. The problem of aggregation was overcome by solubilization of LPS in perdeuterated dihexanoylphosphatidylcholine (DHPC) micelles, which serve as a mimetic of the bacterial membrane. In combination with isotope labeling by ^{13}C and ^{15}N atoms, this makes LPS amenable to a large number of modern heteronuclear solution NMR spectroscopy techniques.

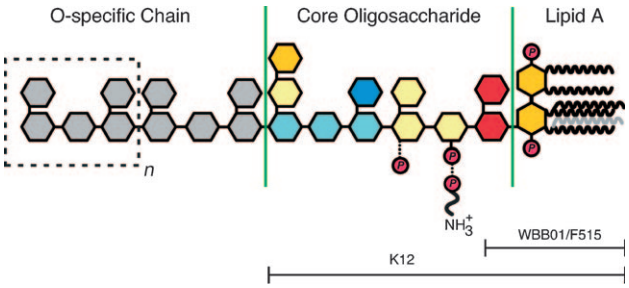

Figure 1. Overall architecture of *E. coli* LPS. Different sugar units are color coded as follows: dark yellow: glucosamine (GN); red: 3-deoxy-D-*manno*-oct-2-ulosonic acid (KD); light yellow: L,D-heptose; light blue: glucose; dark blue: galactose. Fatty acids attached to GN units are shown as wavy lines; phosphate groups are indicated by red circles. Variations in phosphorylation patterns, including a phosphoethanolamine, are indicated by dashed lines. The lengths of LPS expressed by *E. coli* strains K12, WBB01, and F515 are shown as horizontal bars. LPS derived from F515 is predominantly pentaacylated. The respective missing fatty acid is shown in gray.

[*] Dr. W. Wang, Dr. H. J. Sass, Prof. S. Grzesiek[+]
Division of Structural Biology, Biozentrum
University of Basel
Klingelbergstrasse 50/70, 4056 Basel (Switzerland)
E-mail: stephan.grzesiek@unibas.ch
Prof. U. Zähringer[+]
Research Center Borstel, Division of Immunochemistry
Parkallee 4A, 23845 Borstel (Germany)
E-mail: uzaehr@fz-borstel.de
[+] These authors contributed equally to this work.

[**] We would like to thank B. Lindner and H. Moll for expert help with the mass spectrometry analysis, J. Grötzinger for a generous gift of $^{13}C,^{15}N$-labeled bacterial dry mass of *Escherichia coli* K12, and K. Schmengler and U. Schombel for the preparation of $^{13}C,^{15}N$-labeled lipopolysaccharide and lipid A (WBB01 and F515). This work was supported by a stipend from the Roche Research Foundation (to W.W.), the Schweizerische Nationalfonds (grant no. 31-109712; to S.G.), and by the Deutsche Forschungsgemeinschaft (SFB 470, Project B4; to U.Z.).

Supporting information for this article is available on the WWW under http://dx.doi.org/10.1002/anie.200803474.

Highly purified U-$^{13}C/^{15}N$-labeled LPS-6 was obtained from the *E. coli* deep rough mutant WBB01 (details are given in the Supporting Information). This LPS-6 variant consists of lipid A with all six fatty acid chains and two KD sugar units (Figure 2, inset). A number of solvents and detergent systems were tested to solubilize LPS-6. Solubilization in aqueous mixtures of DHPC and dimyristoylphosphatidylcholine (DMPC) proved to be very efficient. Variation of the molar DMPC/DHPC ratios from 0 to 3.1 showed that LPS solubilized by pure perdeuterated DHPC (3% w/v) had the best spectral qualities. NMR relaxation data obtained on the ^{15}N nuclei of the two GN amide groups ($T_1 =$ 0.56 s, 37 °C, 600 MHz) were consistent with a micelle size of about 9 kDa, that is, small enough for most heteronuclear solution NMR spectroscopy experiments. Figure 2 shows an example of a $^{1}H–^{13}C$ HSQC spectrum, which indicates that almost all of the sugar resonances are completely resolved and that the resolution is sufficient to distinguish the fatty acid resonances up to approximately the fourth position along the alkyl chain.

The assignment of the resolved resonances was achieved by a combination of heteronuclear spectra (Figure 3). In brief, unique connections between adjacent $^{1}H–^{13}C$ moieties in the sugar rings and along the fatty acid chains could be established from 3D HCCH-TOCSY and HCCH-COSY experiments. This yielded complete assignments of all sugar $^{1}H/^{13}C$ signals. Subsequently, the fatty acids were easily distinguished and assigned. Thus, 2D versions of protein H(N)CO, CBCA(N)H, and CBCA(CON)H experiments could be used to connect the $^{1}H–^{15}N$ resonances to adjacent ^{13}C nuclei in the GN and FA moieties (Figure 3). For example, the CBCA(N)H experiment (Figure 3) shows correlations of one amide $^{1}H^{N}$ proton with the $^{13}C1$, $^{13}C2$, and $^{13}C3$ signals of GN1. Further crosspeaks are observed to the $^{13}C2$ and $^{13}C3$ signals of FA1; these interactions are corroborated by corresponding resonances in the CBCA(CON)H experiment. This establishes a connection between the resonances of GN1 and FA1. Further connections to other $^{1}H–^{13}C$ resonances along the FA chain, up to the C4 atom, could then be obtained by the 3D HCCH-TOCSY experiment. The assignment of the other FAs followed a similar route, augmented with information from a ^{13}C-edited

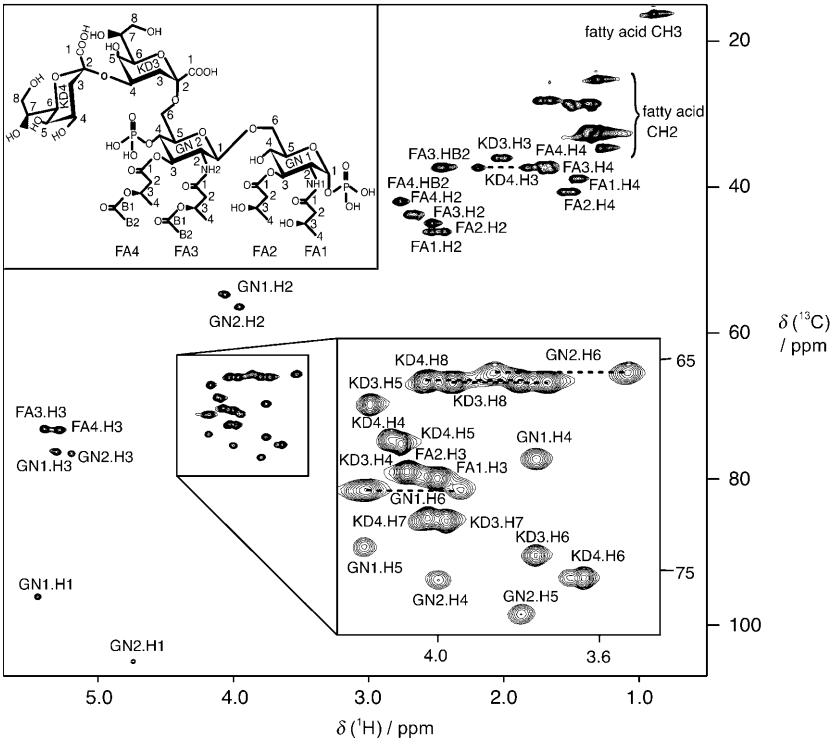

Figure 2. $^{1}H–^{13}C$ HSQC of $^{13}C/^{15}N$-labeled LPS-6 in 3% DHPC at 310 K. Resonances are marked with assignment information. Inset: the chemical structure of LPS-6 with part of the fatty acid side chains shown.

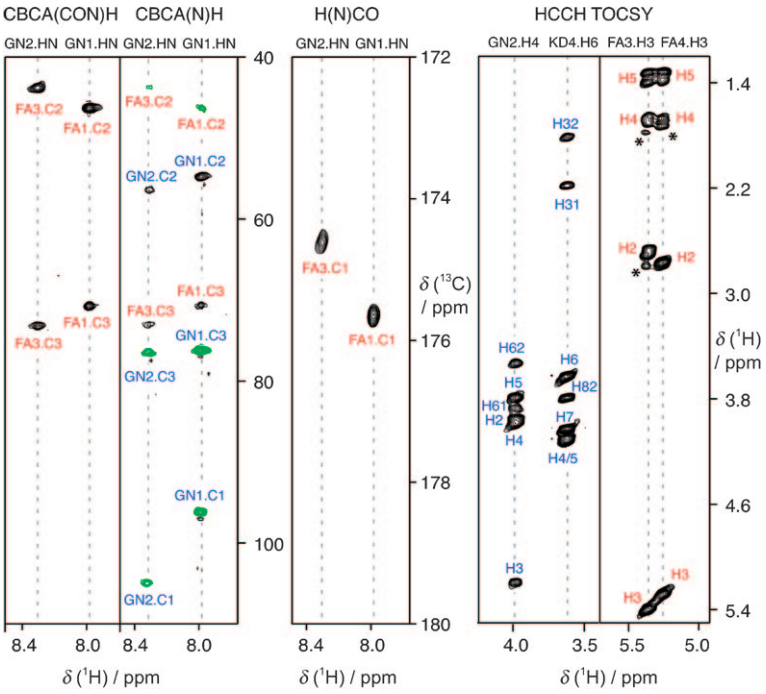

Figure 3. Selected regions from 2D CBCA(CON)H, CBCA(N)H, and H(N)CO, 3D HCCH TOCSY spectra of LPS-6 showing the assignment strategy. Peaks are labeled with assignment information for sugars (blue) and fatty acids (red). Negative resonances of the CBCA(N)H spectrum are shown in green. Vertical dashed lines indicate frequency positions of proton resonances labeled at the top. Resonances marked by asterisks correspond to overlapping signals from adjacent ^{13}C planes.

NOESY experiment for the ester-linked FAs. Beyond positions C4 for FA1–4 and CB2 for FA3/4, resonances could no longer be assigned separately due to degeneracy resulting from the dynamic and disordered state towards the FA chain ends.

Information on the three-dimensional structure of LPS-6 was derived from a total of 94 NOEs collected in ^{13}C- and ^{15}N-edited 3D NOESY experiments and 14 $^{3}J_{HH}$ couplings obtained from a multiquantum ^{13}C-edited quantitative-J experiment.[14] Consistent with previous findings,[15] the vicinal coupling constants (Table 7 in the Supporting Information) indicate that all four GN and KD units of LPS-6 are in the gluco configuration with a respective chair sugar pucker. GN1 is in the α-D configuration ($^{3}J_{H1H2} = 2.7$ Hz), whereas GN2 is in the β-D ($^{3}J_{H1H2} = 9.6$ Hz) configuration. These configurations are corroborated by the intrasugar NOE patterns. Information on the relative orientation of the LPS-6 sugar units was determined from a total of 27 sugar–sugar and sugar–FA NOE contacts. In particular, GN1 shows numerous contacts to FA3, which is consistent with a tilted conformation of GN1 relative to GN2. In contrast to findings with partial lipid A molecules in SDS micelles,[13] no NOEs are observed that would indicate a higher oligomeric state of LPS in the DHPC micelles. This is corroborated, for example, by the size of the micelles obtained from relaxation data. Thus, we conclude that LPS is monomeric in the DHPC micelles.

The LPS/DHPC micelles proved to be amenable to weak alignment in mechanically strained polylacrylamide gels (Figure 1 and Table 8 in the Supporting Information).[16,17] Thus, the conventional NOE and J-coupling structure information could be supplemented by a large number of residual dipolar couplings (RDCs). A total of 38 $^{1}D_{HC}$ ($^{1}D_{HC,max} = 25$ Hz), $^{1}D_{HN}$, and $^{3}D_{HH}$ RDCs were determined, which gave valuable information on the direction, length, and dynamics of the respective internuclear vectors.[18]

The structure of LPS-6 (the fatty acid chains include only atoms up to the C4 atom) was calculated by using the program XPLOR based on the NOE, J-coupling, and RDC data. Since the RDCs showed evidence of internal dynamics, two separate orientation tensors with floating values, according to the ISAC method,[19] were used for the two GN (GN1/2) and the two KD (KD3/4) subunits during the calculation. The choice of only two, instead of four, separate tensors for the four sugar groups was motivated by the requirement for sufficient sampling of all directions of space by the observed RDCs and by the consideration that the relative flexibility of the GN and KD subunits is limited by the lipid anchors and steric constraints, respectively. Indeed for the KD subunits, numerous strong intersubunit NOEs indicate restriction of the rotation around the KD3–KD4 glycosidic linkage. This is corroborated by an analysis with the CHARMM force field[20] (data not shown), which yields only one possible relative orientation between KD3 and KD4, due to steric restriction. This conformation is also completely consistent with the observed NOE pattern.

Figure 4 shows a superposition of the 50 lowest energy structures from the 200 calculated structures. The GN1/2 and KD3/4 subunits are individually very well defined with root mean square deviations (RMSDs) of 0.12 and 0.05 Å for the

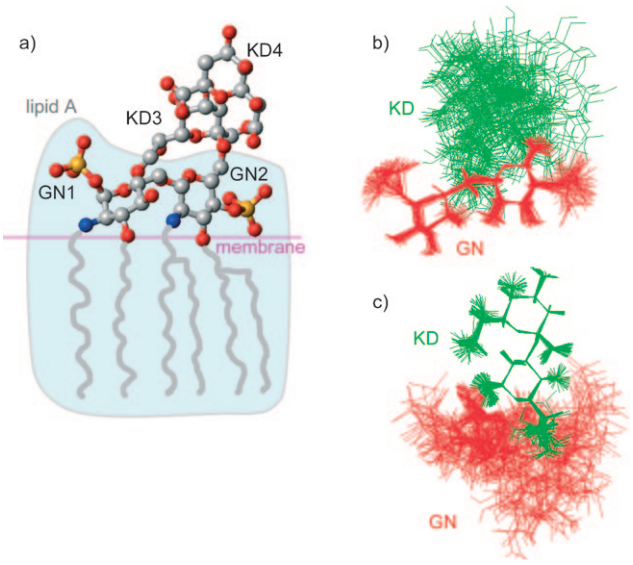

Figure 4. a) The lowest energy structure of LPS-6 with the GN and KD units shown in a ball-and-stick representation and the fatty acid chains shown as a cartoon. The lipid A part of LPS-6, which is responsible for the endotoxic reaction, is highlighted by a pale blue background. The orientation of LPS with respect to the membrane is indicated. b, c) Calculated structure ensemble showing the 50 lowest energy structures with the units of GN1/2 (b) or KD3/4 (c) aligned relative to each other.

carbon atoms of the GN and KD sugar rings, respectively (Table 9 in the Supporting Information). However, the relative orientation between the GN1/2 and KD3/4 subunits is not well defined. An analysis of the GN1/2 and KD3/4 orientation tensors shows that this is not caused by a lack of data but by intrinsic dynamics. Both tensors are well defined with generalized sampling parameters X[21] of 0.14 ($N = 24$) for GN and 0.07 ($N = 14$) for KD ($X = 0$ indicates optimal isotropic sampling and $X = 1$ indicates sampling of only 1 direction of the 3D space; N is the number of RDCs). The generalized degrees of order (GDOs)[22,23] for the GN1/2 and KD3/4 subunits are 35 and 25 Hz, respectively; these values indicate that the KD3/4 subunit is considerably more flexible than the GN1/2 subunit. For example, when interpreted by a wobbling in a cone model, the GDO ratio of 0.65 corresponds to a movement of the KD3/4 subunit relative to the GN1/2 subunit within a cone of opening angle of ±42° during the timescale of the RDC detection, that is, within tens of milliseconds.

The two GN units, including the fatty acids, constitute the endotoxic recognition motif. A comparison of the conformation of the two GN units with the known X-ray structures of LPS in the incidental complex with FhuA[8] and of the LPS-like, four-fatty-acid antiendotoxic lipid IV_A and eritoran molecules in complexes with MD2[9] and MD2/TLR4[10] reveals that the relative orientation of the GN sugar moieties and the direction of the lipid chains are similar (Figure 2 in the Supporting Information). However, the RMSDs between the NMR spectroscopy and X-ray crystallography structures range between 1.1 and 1.7 Å for the two sugar units (Table 10 in the Supporting Information), that is, they are significantly

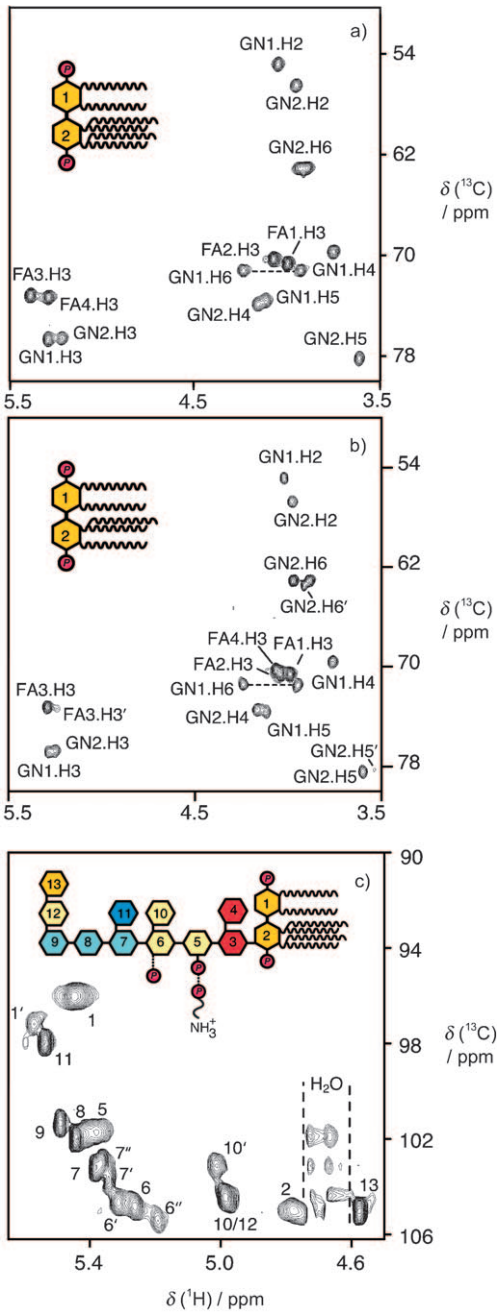

Figure 5. Selected parts of the ^{1}H–^{13}C HSQC spectra of LPS variants A) LA-6, B) LA-5, and C) K12. Sketches of the respective chemical structures are shown in inserts with color coding according to Figure 1. Primes and double primes denote secondary and ternary spectral species that very likely result from chemical heterogeneity.

larger than the RMSD of the NMR spectroscopy structure ensemble. This is caused by considerable deviations of the torsion angles defining the glycosidic linkage (Table 11 in the Supporting Information). We conclude from this phenomenon that the relative orientation of the two GN units is variable and dictated by the molecular context, that is, by the composition of the fatty acids and the binding to receptor molecules. This should have relevance for immune recognition, because the conformation of the LPS molecule may vary during transfer between the receptors of the innate immune system.

The combination of isotope labeling, solubilization by DHPC, and heteronuclear NMR spectroscopy experiments was also used to analyze a variety of other LPS molecules. For example, hexa- and pentaacylated lipid A molecules (LA-6 and LA-5) could be easily distinguished from their ^{1}H–^{13}C HSQC spectra (Figure 5a,b). In LA-5, the ester-linked fatty acid at position FA4.C3 is replaced by a hydroxy group. This leads to a characteristic upfield shift of the FA4.$^{1}H3$–$^{13}C3$ frequency pair (Figure 5b). A more complex LPS molecule is represented by K12 (Figure 5c), which contains 11 additional sugar moieties attached to the lipid A. The resonances are well resolved and the different types of sugars are easily assigned from the described combination of ^{13}C-edited TOCSY and NOESY spectra. A number of heterogeneities are visible, which are caused by, for example, the different phosphorylation patterns described in Figure 1. These different LPS molecular species were not separated during purification from the *E. coli* K12 source. For all of these samples, LA-6, LA-5, and K12, high-quality NOE and RDC data can be obtained.

In summary, we have presented a general method for the structure characterization of complex and even heterogeneous LPS molecules under conditions that mimic the natural environment in the bacterial membrane much more closely than previous attempts.[22,23] In particular, the current method should also be useful for the investigation of complexes of LPS with its cognate receptors.

Received: July 17, 2008
Published online: November 25, 2008

Keywords: isotopic labeling · lipopolysaccharides · membrane mimetics · NMR spectroscopy · structure elucidation

[1] K. M. Choe, T. Werner, S. Stöven, D. Hultmark, K. V. Anderson, *Science* **2002**, *296*, 359–362.
[2] S. D. Wright, R. A. Ramos, P. S. Tobias, R. J. Ulevitch, J. C. Mathison, *Science* **1990**, *249*, 1431–1433.
[3] H. Burchardi, H. Schneider, *PharmacoEconomics* **2004**, *22*, 793–813.
[4] D. C. Angus, W. T. Linde-Zwirble, J. Lidicker, G. Clermont, J. Carcillo, M. R. Pinsky, *Crit. Care Med.* **2001**, *29*, 1303–1310.
[5] U. Zähringer, B. Lindner, E. T. Rietschel in *Endotoxin in Health and Disease* (Eds.: H. Brade, S. Opal, S. Vogel, D. C. Morrison), Marcel Dekker, New York, **1999**, pp. 93–114.
[6] D. R. Dixon, R. P. Darveau, *J. Dent. Res.* **2005**, *84*, 584–595.
[7] H. Loppnow, H. Brade, I. Dürrbaum, C. A. Dinarello, S. Kusumoto, E. T. Rietschel, H. D. Flad, *J. Immunol.* **1989**, *142*, 3229–3238.
[8] A. D. Ferguson, E. Hofmann, J. W. Coulton, K. Diederichs, W. Welte, *Science* **1998**, *282*, 2215–2220.
[9] U. Ohto, K. Fukase, K. Miyake, Y. Satow, *Science* **2007**, *316*, 1632–1634.
[10] H. M. Kim, B. S. Park, J. I. Kim, S. E. Kim, J. Lee, S. C. Oh, P. Enkhbayar, N. Matsushima, H. Lee, O. J. Yoo, J. O. Lee, *Cell* **2007**, *130*, 906–917.
[11] S. M. Strain, S. W. Fesik, I. M. Armitage, *J. Biol. Chem.* **1983**, *258*, 13466–13477.

[12] M. Oikawa, T. Shintaku, H. Yoshizaki, K. Fukase, S. Adachi, K. Lee, S. Kusumoto, *Bull. Chem. Soc. Jpn.* **2001**, *74*, 1455 – 1461.
[13] M. Oikawa, T. Shintaku, N. Fukuda, H. Sekljic, Y. Fukase, H. Yoshizaki, K. Fukase, S. Kusumoto, *Org. Biomol. Chem.* **2004**, *2*, 3557 – 3565.
[14] S. Grzesiek, H. Kuboniwa, A. P. Hinck, A. Bax, *J. Am. Chem. Soc.* **1995**, *117*, 5312 – 5315.
[15] U. Zähringer, V. Sinnwell, J. Peter-Katalinic, E. T. Rietschel, C. Galanos, *Tetrahedron* **1993**, *49*, 4193 – 4200.
[16] R. Tycko, F. J. Blanco, Y. Ishii, *J. Am. Chem. Soc.* **2000**, *122*, 9340 – 9341.
[17] H. J. Sass, G. Musco, S. J. Stahl, P. T. Wingfield, S. Grzesiek, *J. Biomol. NMR* **2000**, *18*, 303 – 309.
[18] N. Tjandra, A. Bax, *Science* **1997**, *278*, 1111 – 1114.
[19] H. J. Sass, G. Musco, S. J. Stahl, P. T. Wingfield, S. Grzesiek, *J. Biomol. NMR* **2001**, *21*, 275 – 280.
[20] B. R. Brooks, R. E. Bruccoleri, B. D. Olafson, D. J. States, S. Swaminathan, M. Karplus, *J. Comput. Chem.* **1983**, *4*, 187 – 217.
[21] D. Fushman, R. Ghose, D. Cowburn, *J. Am. Chem. Soc.* **2000**, *122*, 10640 – 10649.
[22] J. H. Prestegard, H. M. Al-Hashimi, J. R. Tolman, *Q. Rev. Biophys.* **2000**, *33*, 371 – 424.
[23] J. Sass, F. Cordier, A. Hoffmann, A. Cousin, J. G. Omichinski, H. Lowen, S. Grzesiek, *J. Am. Chem. Soc.* **1999**, *121*, 2047 – 2055.

